Protective Effects of Dietary Flavonoid, Apigenin Against Sorafenib-Induced Oxidative, Genetic, and Hepato-Renal Toxicity in Swiss Albino Mice

Deepti Singh
Aligarh Muslim University
Mohammad Afsar Khan
Aligarh Muslim University
Kafil Akhtar
J.N. Medical College, Aligarh Muslim University
Farruk Arjmand
Aligarh Muslim University
Hifzur R Siddique (hifzur.zo@amu.ac.in)
Aligarh Muslim University

Research Article

Keywords: Dietary Flavonoid-Apigenin, Sorafenib, Genotoxicity, Oxidative damages, Hepato-renal toxicity, Amelioration.

Posted Date: March 16th, 2022

DOI: https://doi.org/10.21203/rs.3.rs-1441781/v1

Abstract

Sorafenib is an FDA-approved chemotherapeutic drug used as standard therapy for advanced-stage cancers. However, Sorafenib-induced multiple adverse effects is a major limitation that directly impacts patients' physical and physiological well-being. Therefore, it is vital to identify agents that can lessen the associated adverse effects and enhance efficacy. Apigenin, a dietary plant-flavone, is a bioactive-compound present in fruits and vegetables having anti-oxidant, anti-inflammatory, and anti-cancer properties. Our study aimed to investigate Sorafenib-induced toxic effects at genomic, cellular, and tissue level and the potential protective effects of Apigenin. We performed DNA interaction, genotoxicity, oxidative damages, anti-oxidant activities, liver enzyme levels, and histopathological studies. We demonstrated that Apigenin and Sorafenib bind DNA via electrostatic interaction. Further, Sorafenib induces genetic, oxidative, and tissue damages characterized by an increase in chromosomal-aberrations and micronucleus, reactive oxygen species (ROS) and nitric oxide (NO), oxidative and DNA damage, lipid peroxidation, and hepato-renal damages, and a decrease in antioxidant-enzymes. Interestingly, the Sorafenib-induced adverse effects were ameliorated by Apigenin. Our findings indicate that Apigenin has protective effects against Sorafenib-induced toxicity and could be combined with Sorafenib to lessen its adverse effects and enhance its efficacy. However, further pre-clinical and clinical studies are required to evaluate Apigenin's effectiveness with Sorafenib.

1. Introduction

The potential use of plant-derived compounds (present in fruits and vegetables consumed by humans) as the protectors/attenuators against genotoxic and oxidative damage is gaining widespread attention (Siddique et al. 2011; Maurya et al. 2020). Apigenin, 4',5',7, -trihydroxy flavone (molecular formula $C_{15}H_{10}O_5$) is a common dietary flavonoid abundant in many fruits (such as grapes, apple), vegetables (such as onion, pepper, celery), Chinese medicinal herbs, and beverages (such as tea, wine, beer) (Singh et al. 2019). It has several physiological effects such as anti-oxidant, anti-inflammatory, anti-genotoxic, anti-proliferative, anti-angiogenic, cardiovascular, anti-mutagenic, and anti-cancer (reviewed by Singh et al. 2019). In addition to the above benefits, it also exhibits chemopreventive potential against several cancer types with low intrinsic toxicity (Yan et al. 2017). The anti-proliferative action of Apigenin is exerted via the modulation of cell signaling molecules involved in cell proliferation, invasion, and metastasis. Interestingly, Apigenin selectively induces apoptosis in cancer cells while sparing the normal cells (Yan et al. 2017).

Further, studies have shown that the co-administration of Apigenin with chemotherapeutic drugs such as paclitaxel and cisplatin significantly enhance the anti-cancer efficacy of chemotherapeutic drugs and helps overcome the limitations of chemotherapy (Liu et al. 2017; Pal et al. 2017). To evaluate the prevention of neoplasia recurrence, the pharmacological effects of Apigenin as a dietary supplement are under evaluation in phase 2 clinical study where a bioflavonoid mixture of Apigenin and Epigallocatechin gallate is served as a daily nutritional supplement to colorectal carcinoma patients which have

undergone resection (https://clinicaltrials.gov/ct2/show/NCT00609310). The above evidence guided us to design and explore the protective effects of Apigenin against Sorafenib-induced toxic effects.

Sorafenib/Nexavar is an FDA-approved oral multi-kinase inhibitor developed as a standard line of therapy for advanced liver cancer. It was initially developed as an inhibitor of Raf-1. However, subsequently, it was reported to inhibit the activity of various other kinases involved in tumor progression and angiogenesis, such as VEGFR/2–3, PDGF-R, FLT-3, and c-Kit (Liu et al. 2006). Sorafenib is the first oral agent that has shown activity against human hepatocellular carcinoma (HCC) and has been approved to treat patients with unresectable HCC. However, the efficacy of Sorafenib alone in the treatment of HCC has several adverse effects leading to treatment interruptions, failure, or even death of the patients (Li et al. 2015). The most frequently reported dose-limiting toxicities of Sorafenib include head-foot skin reactions, rash, desquamation, diarrhea, anorexia, nausea, vomiting, arterial hypertension, and fatigue (Li et al. 2015). Among the adverse effects of Sorafenib, hepato-renal toxicity is also a common event leading to the discontinuation of the treatment (Williet et al. 2017). Several researchers attempted to minimize the dose of Sorafenib by combining it with other agents such as Chinese herbal medicines, thereby ameliorating the toxic side effects (Ting et al. 2017). Recent clinical and pre-clinical studies show that phytochemicals exert potential hepatoprotective, immunomodulatory, and antitumor effects. Therefore, there is a need to identify compounds that, in combination with Sorafenib, reduce its toxicity and increase its efficacy.

The main goal of the present study was to analyze whether Apigenin reduces the toxic effects of Sorafenib at the genomic, cellular, and tissue level. To the best of our knowledge, Apigenin appears to have the potential to be used as a dietary supplement and adjuvant chemotherapeutic agent for cancer therapy and show significant protective effects and alleviate the Sorafenib-mediated adverse effects.

2. Materials And Methods

2.1. Chemicals and Reagents

Sorafenib (CAS No. BAY 43-9006; ≥ 99% purity) and Apigenin (CAS No. LY 080400; ≥ 99% purity) was purchased from Selleck Chemicals (USA). Tris (hydroxymethyl) aminomethane and Disodium salt of calf thymus DNA (ct-DNA) was purchased from Sigma Aldrich (USA). DPPH (95% purity) and Colchicine were purchased from SRL (Cat. No. 29128) and Merck, India, respectively. All other reagents/chemicals used in the study were of analytical grade.

2.2. *In vitro* DNA Interaction Studies

2.2.1. Absorption studies

The experimental procedure used for analyzing the interaction of the compounds (Apigenin, Sorafenib, and their combination) with ct-DNA was carried out in an aerated buffer (5 mM Tris-HCl, 50 mM NaCl, pH = 7.2). The Absorption spectral traces with ct-DNA conformed to the standard methods previously adopted by Parveen et al. (2017). The concentration per base pair for ct–DNA was determined

spectrophotometrically by assuming 260 value to be 6600 M^{-1} cm^{-1}, respectively (Marmur and Doty, 1961; Meadows et al. 1993). While measuring the absorption spectra, an equal amount of ct–DNA was added to the compound solution and the reference solution. The binding strength was quantified by intrinsic binding constant; *Kb* value determined using Wolfe–Shimer equation (Wolfe et al. 1987) viz. (DNA)/ $\varepsilon_a - \varepsilon_f$= (DNA)/ $\varepsilon_b - \varepsilon_f + 1/ K_b(\varepsilon_b - \varepsilon_f)$ Where ε_a, ε_f, and ε_b are A_{obsd}/(Compound), extinction coefficient for free compound and extinction coefficient for the compound in the fully bound form, respectively. A plot of (DNA)/($\varepsilon_a - \varepsilon_f$) *vs.* (DNA), where (DNA) is the concentration of DNA in base pairs, gives K_b as the ratio of slope to the intercept.

2.2.2. Fluorescence studies

Fluorescence studies were performed to validate the results of Absorption studies. Binding constant K of the compounds (Apigenin, Sorafenib, and their combination) was determined from Scatchard equations by employing emission titration (Healy, 2007): $C_f = C._T. (I/I - P) (1-P)$; $r/C_f = K (n-r)$ Where C_f is the concentration of free probe, $C._T.$ is the total concentration of added probe, I and I_0 are fluorescence intensities when DNA is present and absent, respectively and P is the ratio of observed fluorescence quantum yield of the bound probe to that of the free probe. The value P was obtained as the intercept by extrapolating from a plot of I/I_o *vs.* 1/(DNA), r denotes the ratio of $C._B.$ (= C.T.–C_f) to the DNA concentration, i.e., the bound probe concentration to the DNA concentration, K is the binding constant and C_f, is the free compound concentration and "n" is the binding site number.

2.2.3. Ethidium bromide displacement assay

An emission quenching experiment was performed to further validate the binding mode of compounds. Briefly, Ethidium bromide (E.B.), the most sensitive probe intercalating between the base pairs, is used. Quenching experiments are based on the decrease in fluorescence intensity when the quencher compound displaces the bound E.B. molecule from the EB-DNA complex. Emission intensity measurements were carried out using Hitachi F–2700 fluorescence spectrophotometer in a 1 cm path length quartz cell.

2.2.4. Confocal microscopy

The intracellular generation of ROS was measured using carboxy-H_2DCFDA, a cell-permeable fluorescent probe. Briefly, Huh7 liver cancer cells were cultured in Dulbecco's modified Eagle's medium (DMEM) supplemented with 10% fetal bovine serum (FBS) and penicillin/streptomycin at 37° C in standard cell culture conditions. 1 x 10^6 liver cancer cells (Huh7) were plated in a 4-well chamber slide and allowed to attach overnight. Cells were then treated with the test chemicals for 24 hrs, and then 5 µM of H_2DCF-DA was added and incubated for 30 mins at 37° C. The cells were finally collected by trypsinization, and DCFDA fluorescence was analyzed using a confocal microscope.

2.3. Experimental design for *in vivo* studies

2.3.1. Animals

This study was conducted on Swiss Albino mice according to the ethical standards and guidelines of the Committee for control and supervision of experiments on animals (CPCSEA). Prior approval was obtained for the experiment protocol from the Institutional Animal Ethics Committee (1979/G.O./Re/S/17/CPCSEA/8). The animals (weighing about 25–30 kg) were housed separately in standard laboratory conditions (room temperature of 18°-25°C; relative humidity of 45–55% and a 12/12h light/dark period) and were fed and provided water daily *ad libitum.* Before starting the experiment, the animals were acclimatized for 15 days.

2.3.2. Groups and treatment

Sorafenib was dissolved in DMSO in a final concentration of 0.1%. Apigenin was dissolved in 90% corn oil and 10% DMSO. After acclimatization, the animals were weighed and randomly divided into four groups of five animals each (Fig. 1). Group-I served as negative control and was fed with the standard diet and treated with corn oil. Group-II was administered with 50 mg/kg of Apigenin intraperitoneally (i.p). Group-III was treated with 40 mg/kg of Sorafenib, i.p, and Group-IV was treated with 50 mg/kg Apigenin (i.p) and 40 mg/kg Sorafenib (i.p).

2.3.3. Blood, Femurs, and Organ collection

At the end of the experiment, the animals were euthanized. Blood was withdrawn from each animal by cardiac puncture and allowed to stand for 30 minutes. Serum was separated from the blood and was stored in -80°C for analysis of serum biochemistry; femurs were used for genotoxicity assay; organs such as liver and kidney were collected and stored at -80°C for oxidative stress and in formalin for histopathological examination.

2.4. Analysis of Genotoxicity

Genotoxic effects of Sorafenib were studied by chromosomal aberration assay and micronucleus test. The genotoxicity assays were done immediately after the animals were sacrificed.

2.4.1. Chromosomal Aberration Assay

Chromosomal preparation was done according to Chauhan et al. (2000) with little modifications (Khan et al. 2022). Briefly, to analyze the test chemical-induced genotoxic effects (if any), we exposed the animals to Apigenin, Sorafenib, and a combination of Apigenin and Sorafenib for the desired period. Before sacrificing the animals, the animals were treated with Colchicine (2 mg/kg) to arrest the cells in the metaphase stage. Animals were sacrificed, and femurs were taken out and flushed with 0.075M KCL 2–3 times to collect the bone marrow. Cells were incubated and centrifuged at 1000 rpm for 5 mins. The supernatant was discarded, and the pellet was resuspended. Cells were then fixed in freshly prepared and chilled methanol: glacial acetic acid (3:1). The sample was centrifuged again, and 2–3 washings were given. The cell suspension was dropped on clean chilled slides, flamed shortly, and stained in Giemsa for 20 mins. Slides were then analyzed under a microscope to score the chromosomal preparations in a blinded fashion. 1000 cells per animal, and thus a total of 5000 cells per animal group were analyzed.

2.4.2. Micronucleus Test (MNT)

The Micronucleus test was done as described before by Chauhan et al. (2000). After treating the animals with Apigenin, Sorafenib, and a combination of Apigenin and Sorafenib for 48 hrs, mice were sacrificed, and femurs were dissected out. The bone marrow of the animals was flushed in fetal bovine serum (FBS) and centrifuged at 1000 rpm for 10 mins. The supernatant was discarded, and the pellet was resuspended in FBS. Smear was prepared on clean glass slides, and then the slides were air-dried stained differentially in May-Gruenwald solution followed by Giemsa stain. Slides were then made permanent by mounting them in DPX and analyzed under a light microscope. 1000 cells per animal, and thus a total of 5000 cells per animal group were analyzed.

2.4.3. Measurement of 8-hydroxy-2-guanosine levels (8-OHdG)

8-OHdG is considered a marker for oxidative damage of DNA and is one of the predominant forms of lesions generated due to ROS. The interaction of free hydroxyl radical with the DNA nucleobases such as guanine results in the formation of 8-OHdG. 8-OHdG levels were measured using a highly sensitive 8-OHdG ELISA kit by Cusabio, Houston, USA. The assay was carried out as per the instructions of the manufacturer. The minimum detectable dose was typically less than 3.12 ng/mL.

2.5. Reactive Oxygen Species (ROS) estimation in liver

Sorafenib-induced production of ROS was estimated according to the protocol of Niknahad et al. (2017) with slight modification (Khan et al. 2022). Briefly, 200 mg of tissue was taken and homogenized using 2 mL Tris-HCL buffer (ice-cold; 40 mM; pH 7.4). 100 µL homogenate was then incubated at 37° C with 2',7'-dichlorofluorescein diacetate (DCFDA) (1 mL 20 µM) diluted 1:200 in Tris-HCL buffer for 40 mins. 100 µL tissue homogenate incubated with 1 mL Tris-HCL buffer (in same conditions) served as the control of tissue autofluorescence. Last, the fluorescence intensity of the control and treated samples was assessed using PerkinElmer LS55 fluorescence spectrophotometer at λex = 485 nm and λem = 400–800 nm.

2.6. Nitric oxide (NO) concentration in the liver

NO concentration in the liver was estimated using Griess Reagent (Somade et al. 2018). The reaction mixture was 50 µL Sulfanilamide, 50 µL of the buffer used in sample preparation, and 50 µL sample. The mixture was incubated for 5 mins, and then 50 µL N-naphthyl ethylenediamine was added, followed by incubation for another 5–10 mins. The absorbance was measured at 540 nm, and the NO concentration was determined with the help of the sodium nitrite standard curve.

2.7. Biochemical Assays

The tissues were homogenized in ice-cold Phosphate-Buffered Saline (PBS), having a pH of 7.4 and Triton x-100 in a ratio of 9:1. The homogenized tissue extract was then centrifuged for 30 mins at 12,000 rpm; the pellet was discarded, and the supernatant was collected to be used for the estimation of enzyme activity.

2.7.1. Measurement of Superoxide Dismutase (SOD) activity (EC 1.15.1.1)

SOD enzymes act as the first line of defense against ROS. SOD enzyme activity was determined by the method of Marklund and Marklund (1974). Briefly, 0.05 M tris-succinate buffer (pH 8.2) was added to the sample, followed by 8.0 mM pyrogallol under dark conditions. Absorbance was read at a wavelength of 412 nm and monitored at every 30 secs in a UV-Vis Spectrophotometer for 3 mins.

2.7.2. Measurement of Catalase (CAT) activity (E.C 1.11.1.6)

CAT activity in tissue extracts was determined by the method described by Cohen et al. (1970). In the U.V. range, H_2O_2 displays a continuous increase in Absorption with a decrease in wavelength. H_2O_2 decomposition can be followed by a decrease in absorbance at 240 nm. Briefly, the sample contains enzyme solution or hemolysate and H_2O_2. The sample is read at a wavelength, 240 nm, and light path, 10 mm. The addition of H_2O_2 starts the reaction.

2.7.3 Measurement of Glutathione peroxidase (GPX) activity (1.11.1.9)

GPx is an enzyme catalyzing the reduction of H_2O_2 and organic hydroperoxides using reduced glutathione (GSH) as the source of reducing equivalents. GPx activity was determined by the method described by Rotruck et al. (1973). If GPx activity is decreased, more hydrogen peroxide is present, which leads to direct tissue damage. The assay mixture contains a solution composed of 0.1M sodium phosphate buffer (pH 7.0), Sodium azide, reduced glutathione, H_2O_2, and 1:10 diluted enzyme extract and water. The tubes are kept at 37°C for 3 mins. Following that 10%, TCA is added, and the mixture is centrifuged at 4°C for 10 mins at 1500 rpm. The supernatant is taken. Disodium hydrogen phosphate and DTNB is added to the supernatant. The absorbance is read at 412 nm against the blank containing DTNB. The enzyme activity was expressed as a microgram of GSH utilized per minute per milligram protein.

2.7.4. Measurement of Glutathione (GSH) level (1.8.1.7)

Glutathione is the primary anti-oxidant defense acting against oxidative damage. GSH levels were determined by the method of Boyne and Ellman (1972). Briefly, the tissue homogenates were mixed with TCA centrifuged for 10 mins at 1500 rpm. After centrifugation, the pellet was discarded, and to the supernatant, Ellman's reagent was added. The absorbance of the reaction mixture was read at 412 nm in a UV-Vis spectrophotometer.

2.7.5. Measurement of Malondialdehyde (MDA) level for Lipid Peroxidation

MDA, a product of lipid peroxidation (LPO) and an indicator of oxidative damage, was determined using the method of Buege and Aust (1978). Liver tissues were homogenized for the assay, and the sample was mixed with TBA-TCA-HCL reagent. The mixture was heated for 20 min and centrifuged at 8500 rpm for 15 min at 4° C. After centrifugation, the absorbance of the pink supernatant was taken at 530 nm in a UV-Vis Spectrophotometer. The results were expressed in nmol of MDA/mL of plasma using a molar extinction coefficient of $1.56 \times 10^{-5}\ M^{-1}\ cm^{-1}$ for the MDA-TBA colored complex.

2.8. DPPH Radical Scavenging activity assay/Anti-oxidant activity

DPPH radical scavenging activity was analyzed in the liver and kidney tissues. The micro-assay was performed according to Norma et al.'s (2014) method. In brief, 2.5 mg DPPH was dissolved in 5 mL methanol (≈ 1.27 mM). This stock solution was freshly prepared, used for measurements, and kept in the dark at ambient temperature when not used. In micro-assay, the final volume was adjusted to 200 µL (193 µL of DPPH-methanol and 7 µL of the anti-oxidant sample). The absorbance of the DPPH-antioxidant was read at 517 nm in a microplate reader. The percent radical scavenging capacity was calculated by the following equation:

Radical scavenging capacity (%)= $(A_{blank} - A_{sample})/A_{blank} \times 100$

2.9. Analysis of serum liver function marker levels

The levels of AST (EC 2.6.1.1), ALT (E.C 2.6.1.2), and ALP (3.1.3.1) were estimated using the commercial colorimetric assay kits and according to the protocol of the manufacturer to analyze the effect of Apigenin, Sorafenib and their combination on the functioning of the liver.

2.10. Histopathological examination of liver and kidney

Gross and histopathological examination of liver and kidney were done according to the method of Gray (1954). After sacrificing the animals, the liver and kidney were taken out and rinsed in ice-cold phosphate-buffered saline (PBS). The liver and kidney tissues were fixed in 10% formalin. The formalin-fixed tissues were then dehydrated in grades of alcohol, embedded in paraffin wax, and sectioned in a thickness of 5 µm. The sections were then placed on a clean glass slide pre-coated with glycerol and albumin to stick the sections and deparaffinized, rehydrated, and then stained with Haematoxylin and Eosin (H and E) stain. The slides were then observed under the microscope for any gross abnormalities, and the histo-morphological changes were tabulated for each slide.

2.11. Statistical analysis

Before analysis, normal distribution of data and homogeneity of variance were tested. All the data are presented as the mean ± S.D. The data were analyzed using One-Way Analysis of Variance (ANOVA) followed by Tukey's post hoc test for multiple comparisons were done with the help of the statistical software GraphPad Prism 9.0 (C.A., U.S.). The level of significance was set at $P < 0.05$.

3. Results

3.1. *In vitro* DNA binding studies

3.1.1. Absorption spectral studies

The absorption titration technique is one of the most standard ways to determine the compound's intrinsic binding constant (K_b) and the mode of interaction with ct-DNA by monitoring the absorption bands. Upon progressive titration of compound Apigenin, Sorafenib, and combination of Apigenin and Sorafenib (6.66 x 10^{-6} M) with aliquots of ct-DNA (0.00-3.33 x 10^{-5} M), 'hyperchromism' was observed in wavelength (Fig. 2A-C). The 'hyperchromism' is generally associated with non-covalent interactions *via an* electrostatic mode of binding and the breakage of hydrogen bonds that stabilize the secondary structure of nucleic acids (Gupta et al. 2013). Based on the experimental observations, we presume an electrostatic mode of binding between compounds Apigenin, Sorafenib, and a combination of Apigenin with Sorafenib and ct-DNA.

The quantitative assessment of the binding propensity of Apigenin, Sorafenib, combinations of Apigenin and Sorafenib towards ct-DNA was done by calculating intrinsic binding constant, K_b values by using the Wolfe–Shimer equation, which was found to be- Apigenin = 2.78 x 10^5 M^{-1}; Sorafenib = 1.54 x 10^6 M^{-1} ; Apigenin + Sorafenib = 5.50 x 10^5 M^{-1}.

3.1.2. Fluorescence spectral studies

In the absence of ct-DNA, the compound did not exhibit any luminescence in Tris-HCl buffer at ambient temperature with a maximum wavelength at ~ 390 nm when excited at 270 nm. Upon progressive addition of ct-DNA to the compound, the fluorescence-emission intensity was enhanced, indicating that the compound interacted strongly with DNA. The observed higher emission intensity was attributed to decreased vibrational modes of relaxation due to restricted complex mobility at the binding site, which could be due to the inaccessibility of the solvent molecules to reach the hydrophobic environment inside the DNA helix (Tan et al. 2007).The binding constant, *K* values of the compound with ct-DNA were found to be- Apigenin = 7.08 x 10^5 M^{-1}; Sorafenib = 5.67 x 10^6 M^{-1}; Apigenin + Sorafenib = 3.18 x 10^5 M^{-1} (Fig. 2D-F).

3.1.3. Ethidium bromide displacement assay/Quenching experiments

Emission quenching experiments were also carried out with E.B., the most sensitive fluorescence probe that can intercalate between adjacent base pairs of double-stranded DNA (Raja et al. 2005). The phenomenon could be due to the competition of the compounds with E.B. for the same binding sites on DNA, resulting in the knockout of E.B. from DNA. The titration of the DNA–E.B. system with compound displayed a decrease in emission intensity of the DNA-EB system as depicted in (Fig. 2G-I). It can be inferred from the decrease in emission intensity that there could be partial intercalation of the aromatic

moiety into the DNA helix, as complete intercalation results in the enhancement of the emission intensity. The observed results implicate that the compound caused the contraction of DNA *via* the electrostatic binding mode (Kang et al. 2005). The quenching extents (*Ksv*) of the compound with ct-DNA were determined qualitatively by employing the Stern-Volmer equation and were found to be- Apigenin **=** 0.84; Sorafenib = 1.0; Apigenin + Sorafenib = 0.76.

3.2. Effects of treatment on animal survival, body weight, and liver weight

The present study's findings displayed no significant change in the survival between the treated groups. All the animals survived by the end of the study. The body and liver weights of animals belonging to the groups treated with Apigenin and a combination of Apigenin and Sorafenib did not change significantly compared to control. However, the animals treated with Sorafenib showed a slight and insignificant decrease in body viz-a-viz liver weight compared to control by the end of the study (Fig. 3A & 4I).

3.3. Combination treatment of Apigenin with Sorafenib significantly reduces the Sorafenib-induced Chromosomal Aberrations (CA).

The effect of Apigenin, Sorafenib, and combination of Apigenin with Sorafenib on C.A. was studied in the test animals. The control group of animals showed a mean number aberration of 1.16 ± 0.75. The Apigenin-treated group showed no significant difference in the mean number of CA (1.5 ± 0.83) compared with the control. The Sorafenib-treated group showed a significantly ($P < 0.05$) increased value (11.33 ± 1.63) of C.A. with an approximately ten-fold increase compared to the control. Interestingly, treatment of the animals with a combination of Apigenin and Sorafenib showed a protective effect of Apigenin on the Sorafenib induced genotoxic effects, which were revealed by a significant reduction in the mean number of CA (8.6 ± 2.16) when compared with Group III (Sorafenib alone) (Fig. 3B).

3.4. Combination treatment of Apigenin with Sorafenib significantly reduces the Sorafenib induced micronucleus (MN) production

The effect of Apigenin, Sorafenib, and a combination of both on the micronucleated polychromatic erythrocytes (MNPCEs) were studied. The results demonstrated a mean number of 1.33 ± 0.81 MNPCEs in the control and Apigenin-treated group (1.66 ± 0.51). However, a statistically significant ($P < 0.05$) increase in the mean number of MNPCEs (8.16 ± 1.47) was observed in the Sorafenib-treated group compared to the control. Interestingly, treatment with a combination of Apigenin and Sorafenib demonstrated a protective effect against the Sorafenib-induced production of MNPCEs, which is indicated by a significant reduction in the mean number of MNPCEs (5.5 ± 1.04) on combination treatment (Fig. 3C**-Div**).

3.5. Combination treatment of Apigenin with Sorafenib reduced the 8-OHdG levels

The levels of 8-OHdG were found to be 1.69 ± 0.32, 1.71 ± 0.34, 3.93 ± 0.37, 2.286 ± 0.34 for control, Apigenin, Sorafenib, and combination treatment. Sorafenib treatment caused a significant ($P < 0.05$) increase (~ 132%) in the level of serum 8-OHdG when compared to the control group, indicating oxidative DNA damage. On the other hand, when Apigenin was given in combination with Sorafenib, the levels of 8-OHdG were significantly ($P < 0.05$) reduced (~ 42%), showing the protective effects of Apigenin (Fig. 3E).

3.6. Combination treatment of Apigenin with Sorafenib significantly reduces the Sorafenib induced lipid damage

Further, MDA, an indicator of lipid damage, also supports an increase in the generation of free radicals confirming the depletion of anti-oxidant enzyme activity. The MDA levels were found to be 0.012 ± 0.001, 0.006 ± 0.001, 0.090 ± 0.008, and 0.070 ± 0.009 for control, Apigenin, Sorafenib and combination treatment. The present study's findings revealed an increase in lipid damage suggested by a statistically significant increase (~ 7 folds) in the MDA levels of the Sorafenib-treated group when compared to the control. Further, the protective effect of Apigenin was also demonstrated by a statistically significant decrease (~ 22%) in the MDA levels in the group treated with a combination of Apigenin and Sorafenib. However, no significant difference in the MDA level was observed in the Apigenin-treated group and the control (Fig. 3F).

3.7. Combination treatment of Apigenin with Sorafenib protects against the Sorafenib induced Reactive oxygen species (ROS) and Nitric oxide (NO) production

ROS estimation in the liver was done by analyzing the fluorescence intensity of blank and treated samples. Sorafenib treated group demonstrated the highest fluorescence intensity depicting the highest ROS activity. The highest peak was obtained at 525 nm, nearly 10 folds compared to control. Interestingly, the combination-treated group showed an ~ 42% decrease in the fluorescence/ROS intensity. However, no significant difference was observed in the control and Apigenin-treated groups (Fig. 3G). A similar pattern was observed with the Confocal microscopy in *in vitro* condition (Fig. 3H). Therefore, the present result demonstrates that Apigenin scavenges a significant level of ROS in the combination-treated group. Similarly, Sorafenib treatment also showed a statistically significant ($p < 0.05$) increase in the liver NO concentration (3.90 ± 0.001) when compared with control (1.87 ± 0.002). However, the co-administration of Apigenin and Sorafenib resulted in a significant ($p < 0.05$) reduction in the NO concentration (2.80 ± 0.001). An insignificant difference was observed in the NO concentration between control and Apigenin-treated groups (1.98 ± 0.002) (Fig. 3I).

3.8. Combination treatment of Apigenin with Sorafenib significantly replenishes the anti-oxidant enzyme activity

The endogenous anti-oxidant enzymes such as SOD, CAT, GSH, and GPx are responsible for counteracting the free radicals generated due to oxidative stress. Depletion in the activity of these enzymes might be indicative of enhanced free radical production.

3.8.1. Change in SOD activity in response to Apigenin, Sorafenib, and combination

The SOD enzyme activity was found to be 10.09 ± 0.675, 9.81 ± 0.729, 2.87 ± 0.90, and 6.82 ± 1.14 for control, Apigenin, Sorafenib, and combination (Apigenin + Sorafenib) treatment. The present study revealed that the levels of enzymatic anti-oxidants decreased significantly in the Sorafenib treated group (~ 71%) compared with the control. Interestingly, on treating the animals with a combination of Apigenin and Sorafenib, the enzyme status was found to significantly increase (~ 137%), suggesting the potential of Apigenin in restoring the changes in the enzyme activity towards normal by its anti-oxidant activity. However, no significant difference was observed in the Apigenin and Combination treated groups (Fig. 4A).

3.8.2. Change in CAT activity in response to Apigenin, Sorafenib, and combination

The CAT enzyme activity were found to be 0.0139 ± 0.0008, 0.0131 ± 0.001, 0.006 ± 0.0009, and 0.011 ± 0.001 for control, Apigenin, Sorafenib and combination (Apigenin + Sorafenib) treatment. Our findings reveal a statistically significant ($P < 0.05$) depletion in the CAT enzyme activity in the Sorafenib treated group (~ 56%) when compared with the control. Further, the anti-oxidant potential of Apigenin was also revealed indicative of a statistically significant increase (~ 83%) in the CAT enzyme activity on co-treatment with Apigenin and Sorafenib. However, no significant difference in the CAT enzyme activity was observed in the animals belonging to the Apigenin and combination-treated group (Fig. 4B).

3.8.3. Change in GPx activity in response to Apigenin, Sorafenib, and combination

The GPx enzyme activity were found to be 0.195 ± 0.026, 0.188 ± 0.0156, 0.056 ± 0.017, and 0.144 ± 0.012 for control, Apigenin, Sorafenib and combination treatment. According to the present study's findings, a statistically significant decrease in the GPx enzyme activity was observed in the Sorafenib treated group (~ 71%) compared to the control. Interestingly, the administration of Apigenin along with Sorafenib showed a protective effect of Apigenin against the Sorafenib-induced oxidative damage, which is demonstrated by a statistically significant increase (~ 157%) in the GPx enzyme activity when compared with the Sorafenib treated group. However, the Apigenin and combination-treated groups did not significantly differ in the enzyme activity (Fig. 4C).

3.8.4. Change in GSH in response to Apigenin, Sorafenib, and combination

The GSH levels were found to be 1.156 ± 0.106, 1.106 ± 0.088, 0.516 ± 0.109, and 0.882 ± 0.072 for control, Apigenin, Sorafenib and combination treatment. The present study results demonstrated a statistically significant decrease (~ 53%) in the GSH content in the liver tissues of the Sorafenib-treated group of animals compared to the control. Nevertheless, the GSH content increased significantly (~ 71%) in the liver tissues of the group treated with a combination of Apigenin and Sorafenib, suggesting the hepatoprotective effects of Apigenin by improving the anti-oxidant enzyme capacity. However, the Apigenin and the combination-treated group did not show a significant change in the GSH content (Fig. 4D).

3.9. DPPH Scavenging efficiency/Anti-oxidant potential of Apigenin

DPPH radical scavenging capacity (%) in the liver and kidney tissues is represented in Table 1. The Apigenin-treated group demonstrated maximum scavenging activity in both liver and kidney, followed by the combination-treated group. However, the Sorafenib treated group demonstrated a statistically significant ($p < 0.05$) decrease in the radical scavenging activity as compared to other groups (Fig. 4E-H). The results demonstrate the anti-oxidant potential of Apigenin and its efficacy in ameliorating the Sorafenib-induced oxidative damage in the combination treatment via scavenging the free radicals.

Table 1
The % DPPH Scavenging activity of control, Apigenin, Sorafenib and Combination treated groups at 20 g/mL concentration.

Treatment Groups	**% DPPH ACTIVITY**		
Liver	**0 min**	**15 min**	**30 min**
Control	12.73 ± 0.025	12.26 ± 0.020	10.32 ± 0.016
Apigenin	18.05 ± 0.018*	16.52 ± 0.018*	13.01 ± 0.020*
Sorafenib	1.12 ± 0.003$^{*\#}$	0.64 ± 0.008$^{*\#}$	0.41 ± 0.001$^{*\#}$
Apigenin + Sorafenib	11.80 ± 0.021$^{*\#\$}$	11.58 ± 0.008$^{*\#\$}$	10.29 ± 0.017$^{*\#\$}$
Kidney	**0 min**	**15 min**	**30 min**
Control	10.97 ± 0.018	7.48 ± 0.023	4.60 ± 0.0178
Apigenin	21.14 ± 0.025*	17.00 ± 0.022*	7.88 ± 0.020*
Sorafenib	3.09 ± 0.006$^{*\#}$	2.25 ± 0.008$^{*\#}$	1.93 ± 0.005$^{*\#}$
Apigenin + Sorafenib	11.93 ± 0.017$^{*\#\$}$	10.29 ± 0.008$^{*\#\$}$	6.59 ± 0.01$^{*\#\$}$

3.10. Combination treatment of Apigenin with Sorafenib restores the serum biochemical parameters towards normal

AST, ALT, and ALP are the serum liver function markers. The present study's findings revealed that the exposure of mice to Sorafenib resulted in liver damage, which was suggested by elevated levels of AST, ALT, and ALP compared with the control and Apigenin-treated group. Further, Apigenin showed a protective role against the Sorafenib-induced hepatotoxic effects by bringing a statistically significant decrease in AST, ALT, and ALP levels. However, there was no significant difference in the serum AST, ALT, and ALP levels in the animals belonging to the group treated with Apigenin alone when compared with control (Fig. 4J-L).

3.11. Combination treatment of Apigenin with Sorafenib significantly reduces the Sorafenib induced cytoarchitectural changes in the liver

Sorafenib is primarily metabolized in the liver and undergoes oxidative metabolism mediated by cytochrome P450 (CYP3A4) and glucuronidation through UDP-glucuronosyl transferase (UGT) 1A9 (Tao et al. 2020). The pharmacokinetics of Sorafenib compelled us to observe the effects of Sorafenib on the liver. Histopathological examination of liver sections of the control group (Group I) stained with H&E showed normal hepatic lobules with plates of hepatocytes radiating from the central vein towards the periphery of the lobule. Further, hepatic sinusoids between the adjacent plates were also observed (Fig. 5A-B). The liver sections of the Apigenin treated group (Group II) also showed the histological features of the normal liver with the normal central vein (CV) and portal tract (P.T.) with normal hepatocytes in the cords and normal sinusoidal spaces (Fig. 5C-D).

In contrast, the sections of the liver from the Sorafenib treated group (Group III) showed moderately dilated and congested central vein (CV) (2+). The sections also displayed mildly dilated sinusoids (S) (1+) and mild necrosis of the hepatocytes (N). Further, moderately congested foci of sinusoids (S_1) (2+) and mild hepatocytic vacuoles (V) (1+) were also observed in this group. It also revealed mild diffused acute inflammation when compared with the control (I) (1+) (Fig. 5E-F).

Interestingly, the protective effects of Apigenin on the Sorafenib-induced abnormalities in the liver histology were evidenced in the present study as the group treated with a combination of Apigenin and Sorafenib (Group IV) showed a reduction in the severity of lesions in the liver. The liver sections showed restoration of the normal histology with normal central vein having less diffused hepatocytic vacuoles (1+) and mildly congested sinusoids (S) (1+). No necrosis was observed in this group of animals, and it also revealed reduced diffused acute inflammation (Fig. 5G-H).

3.12. Combination treatment of Apigenin with Sorafenib significantly reduces the Sorafenib induced cytoarchitectural changes in the kidney

The pharmacokinetics of Sorafenib (about 19% elimination by the kidney) compelled us to observe the effects of Sorafenib on the kidney (Lathia et al. 2006). Histopathological examination of the kidney section of the control group (Group I) stained with H&E revealed glomeruli's normal structure and normal proximal and distal tubules (Fig. 6A-B). The kidney sections of the Apigenin-treated group (Group II) also revealed the histological features of a normal kidney with a normal structure of glomeruli (G). Also, the

proximal and distal tubules revealed a cuboidal lining with foci of mild interstitial congestion (C) (Fig. 6C-D).

In contrast, the sections of the kidney from the Sorafenib treated group (Group III) showed moderate glomerular congestion (G) (2+). Also, the sections had mild to moderate necrosis (N) 1 + to 2+. Moderate hemorrhage (H) (2+) was also seen in the sections with a moderate level of interstitial congestion (C) (2+). Also, atrophic changes were observed with focally atrophied tubules (T) with tubular cords (T.C.) (Fig. 6E-F).

Interestingly, the protective effects of Apigenin on the Sorafenib-induced abnormalities in the kidney histology were evidenced in the present study as the group treated with a combination of Apigenin and Sorafenib (Group IV) showed a reduction in the severity of lesions in the kidney. The kidney sections showed restoration of the renal histology towards normal. However, mild glomerular congestion (G) (1+) with mild hemorrhage (H) (1+) was observed. This group also revealed a reduction in the interstitial congestion from moderate to mild (C) (1+) and less focally atrophied tubules (T) (Fig. 6G-H). The results of histopathological examination of the liver and kidney are summarised in Table 2.

Table 2
Results of histopathological examination of liver and kidney in the animals exposed to the test chemical for 48 hrs.

S.No.	Histo-morphological changes	Treatment Groups			
		Control	Apigenin	Sorafenib	Apigenin + Sorafenib
Liver					
1	Dilated and congested central vein (CV)	0/5	0/5	$3/5^{2+}$	0/5
2	Dilated sinusoids (S)	0/5	0/5	$4/5^{1+}$	0/5
3	Necrosis of the hepatocytes (N)	0/5	0/5	$4/5^{1+}$	0/5
4	Congested foci of sinusoids (S_1)	0/5	0/5	$4/5^{2+}$	$2/5^{1+}$
5	Hepatocytic vacuoles (V)	0/5	0/5	$4/5^{1+}$	$2/5^{1+}$
5	Diffused acute inflammation	0/5	0/5	$4/5^{1+}$	$3/5^{1+}$
Kidney					
1	Glomerular congestion (G)	0/5	0/5	$4/5^{2+}$	$1/5^{1+}$
2	Necrosis (N)	0/5	0/5	$4/5^{1+, 2+}$	0/5
3	Interstitial haemorrhage (H)	0/5	0/5	$3/5^{2+}$	$1/5^{1+}$
4	Interstitial congestion (C)	0/5	$2/5^{1+}$	$3/5^{2+}$	$2/5^{1+}$
5	Focally atrophied tubules (TC)	0/5	0/5	$3/5^{2+}$	$2/5^{1+}$
$^{1+}$ mild $^{2+}$ moderate; N = 5 photos for each group					

4. Discussion

Recently, plant-derived natural compounds or phytochemicals are gaining increasing importance (due to their wide availability, low toxicity, and safety) to analyze their protective effects against drug-induced toxicity. In the present study, experiments were performed to screen whether Apigenin has any potential preventive effects against the Sorafenib-induced toxicity. Sorafenib has been used to treat liver and renal cancer for years. Despite its excellent treatment efficacy, Sorafenib-induced toxicity is becoming a key issue limiting its use by oncologists. Frequent exposure to Sorafenib is associated with severe toxicities, including hepatotoxicity and diarrhea, which reduce patients' quality of life, leading to the discontinuation of the treatment. In fact, in 44% of Sorafenib-treated patients in Phase II trials of HCC, the treatment was discontinued due to severe toxicities such as hepatotoxicity and gastrointestinal adverse events (Llovet et

al. 2008). Therefore, the use of adjuvants that might work synergistically to reduce toxicity and increase treatment efficacy is highly recommended. To the best of our knowledge, this is the first study investigating the protective effects of a dietary flavonoid Apigenin using both *in vitro* and *in vivo* conditions against the Sorafenib-induced toxic effects.

Absorption studies showed a hyperchromic effect associated with non-covalent interactions, implicating an electrostatic mode of binding between compounds (Apigenin, Sorafenib, and a combination of Apigenin with Sorafenib) and ct-DNA. The electrostatic binding mode was further substantiated by fluorescence studies, which showed an enhanced fluorescence-emission intensity indicating the strong interaction of the compound firmly with DNA. Further, quenching experiments with E.B. displayed a decrease in emission intensity of the DNA-EB, which also supports the electrostatic interaction between compounds and ct-DNA.

The liver weight, body weight, and liver-to-body weight ratio in the control and Apigenin treated group showed no significant differences suggesting that Apigenin does not affect the animal's health. The genotoxicity assays revealed that Sorafenib had a statistically significant mutagenic effect on the chromosomes, indicating an increase in the mean number of chromosomal aberrations and micronuclei. However, the combination treatment with Apigenin and Sorafenib showed a preventive and protective effect of Apigenin as indicated by a decrease in the mean number of chromosomal aberrations and micronuclei, thus confirming the anti-genotoxic/protective effects of Apigenin. Though Apigenin alone showed insignificant mild genotoxic effects, it demonstrated improved therapeutic/anti-genotoxic effect when given in combination with Sorafenib, possibly targeting different pathways (Das et al. 2013; Singh et al. 2019). 8-OHdG is one of the common adducts formed due to oxidative DNA damage and is a reliable marker for DNA damage (Chao et al. 2021). High serum levels of 8-OHdG are associated with mutagenic effects, and mutations associated with 8-OHdG also reflect the total ROS-mediated damage in DNA. The current study revealed a high level of serum 8-OHdG in mice treated with Sorafenib, which indicates test chemical-induced DNA damage, reduced when the animals were treated with a combination of both the chemicals.

Various studies and growing evidence report that elevated ROS levels help maintain the oncogenic phenotype of cancer cells via acting as the secondary messenger in the intracellular signaling cascade and promote many aspects of carcinogenesis (Liou and Storz, 2014). Further, elevated ROS level is accompanied by the suppression of anti-oxidant enzymes, resulting in malignant transformation via different molecular targets (Bousquet et al. 2019). In addition, the diet rich in anti-oxidants scavenges different kinds of ROS, thereby preventing cancer development (Storz., 2005). In our study, the Sorafenib treated group also revealed maximum ROS intensity depicting the Sorafenib-induced toxicity mediated via the formation of ROS. Multiple experiments demonstrate that ROS-mediated toxicity appears to be alleviated by Apigenin via an anti-oxidant mechanism that protects against oxidative damage. NO is known to be cytotoxic and involved in cell-killing mediated by a necrotic process, either itself or via the formation of peroxynitrite with superoxide anion (Islam et al. 2015). Our results show that the NO concentration is higher in the Sorafenib-treated group. Interestingly, our data also showed the protective

role of Apigenin against the Sorafenib-induced NO production as indicated by the reduction of NO concentration in the combination-treated group.

In the Sorafenib treated group, the weight of the liver and body along with the liver-to-body weight ratio was insignificantly/slightly lower when compared with control. This might be due to the toxic effects of Sorafenib on the liver, which were confirmed in the present study by the histopathological examinations and oxidative stress markers. In general, chemotherapy-induced liver toxicity is one of the most common adverse effects in cancer patients. As we know, Sorafenib is primarily metabolized in the liver and undergoes oxidative metabolism mediated by cytochrome P450 (CYP3A4) and glucuronidation through UDP-glucuronosyl transferase (UGT) 1A9 (Tao et al. 2020). The administration of Sorafenib activates CYP34A, which results in ROS production and subsequently generates oxidative stress and liver injury. Our study revealed an increased level of serum liver function markers, thus suggesting the hepatotoxic effects of Sorafenib. The enhanced marker levels might also be due to cell membrane leakage and loss of hepatocytes (Macgill, 2016).

Further, administration of Apigenin resulted in recovering the levels of these markers suggesting the possible hepatoprotective role of Apigenin which can prevent the liver cells from chemotherapy-induced injury and relieve the severity of liver damage. Further, the liver and kidney's histopathological analysis also revealed the protective effects of Apigenin against the Sorafenib-induced hepato-renal toxicity. These results agree with the study done by Wang et al. (2017), where Apigenin exerts its hepatoprotective effects against alcohol-induced liver injury and cisplatin-induced nephrotoxicity in mice (Hassan et al. 2017). In conclusion, our findings suggest the potential protective role of Apigenin against Sorafenib-induced genotoxic, oxidative, hepatotoxic, and renal toxic effects. With more evidence and extensive studies, it appears to have the potential to be developed as a dietary supplement or as an adjuvant with chemotherapeutic agents.

5. Conclusion

To the best of our knowledge, this is the first study demonstrating the protective effect of Apigenin against the toxicity induced by Sorafenib. Taken together, we conclude that Apigenin plays a protective role against Sorafenib-induced genotoxic, oxidative damage, hepato-renal toxicity. Apigenin attenuated the Sorafenib-induced aberrations in chromosomes and the production of micronuclei. Also, Apigenin efficiently improved the functioning of the liver by improving the levels of liver function markers, anti-oxidant enzymes, and decreasing oxidative damages. This protective effect of Apigenin might result from enhanced anti-oxidant property and inhibition of ROS production. From our study, we proposed a mechanism of Sorafenib-induced toxicity and the protective effects of Apigenin (Fig. 7). These findings may help develop Apigenin-based therapeutics to lessen the Sorafenib-induced adverse effects. Although we observed a promising protective effect of Apigenin against Sorafenib-induced toxicity, the exploration of the protective mechanism is still at a downstream level. It requires further studies to investigate the exact mechanism of action of Apigenin in the reduction of toxic effects. We suggest that it might have the potential to be used as a newer therapeutic application in the future.

Abbreviations

FDA
Food and Drug Administration
VEGFR
Vascular Endothelial Growth Factor Receptor
PDGF-R
Platelet-Derived Growth Factor Receptors
DPPH
2,2-diphenyl-1-picrylhydrazyl.
DCFDA
Dichlorodihydrofluorescein Diacetate
DMSO
Dimethyl Sulfoxide
KCL
Potassium chloride
DPX
Dibutyl Phthalate
MNPCEs
Micronucleated Polychromatic Erythrocytes
8-OHdG
8-Hydroxy-2'-deoxyguanosine
SOD
Superoxide Dismutase
CAT
Catalase
GPx
Glutathione Peroxidase
GSH
Glutathione
AST
Aspartate Aminotransferase
ALT
Alanine Aminotransferase
ALP
Alkaline Phosphatase
MDA
Malondialdehyde

Declarations

Acknowledgments

We would like to thank the Department of Zoology, Aligarh Muslim University, India, for providing the necessary facilities. We also acknowledge Dr. Sabiha Parveen for her assistance in DNA interaction studies.

Authors contributions:

Development of methodology: D. Singh, M.A. Khan, H.R. Siddique

Acquisition of data: D. Singh, M.A. Khan, F. Arjmand, H.R. Siddique

Analysis and interpretation of data: D. Singh, M.A. Khan, K Akhtar, F. Arjmand, H.R. Siddique

Writing of the manuscript: D. Singh, M.A. Khan, H.R. Siddique

Conception and Supervision: Hifzur R Siddique

Funding:

The work was funded byUGC-India (Grant no. F.30-377/2017(BSR)) and DST-SERB, India (Grant no. EMR/20l7/001758), New Delhi, to HRS. Authors (DS and MAK) also express their gratitude to UGC-India (524/ (CSIR-UGC NET JUNE 2019)) and CSIR-India (09/112(0599)/2018-EMR-I) for providing Fellowships, respectively.

Ethics approval:

This study was conducted on Swiss Albino mice according to the ethical standards and guidelines of the Committee for control and supervision of experiments on animals (CPCSEA). Prior approval was obtained for the experiment protocol from the Institutional Animal Ethics Committee (1979/G.O./Re/S/17/CPCSEA/8).

Consent to participate:

Not Applicable

Consent for publication:

All authors have participated in the planning, execution, and analysis of the study and have read and approved this submitted version. The authors declare no conflict of interest.

Availability of data and material (data transparency):

Yes

Code availability (software application or custom code):

Not Applicable

References

1. Bousquet PA, Meltzer S, Sønstevold L, Esbensen Y, Dueland S, Flatmark K, et al. Markers of Mitochondrial Metabolism in Tumor Hypoxia, Systemic Inflammation, and Adverse Outcome of Rectal Cancer. Transl Oncol. 2019 Jan;12(1):76-83.
2. Boyne AF, Ellman GL. A methodology for analysis of tissue sulfhydryl components. Anal Biochem. 1972 Apr;46(2):639-53.
3. Buege JA, Aust SD. Microsomal lipid peroxidation. Methods Enzymol. 1978;52:302-10.
4. Chao MR, Evans MD, Hu CW, Ji Y, Møller P, Rossner P, et al. Biomarkers of nucleic acid oxidation - A summary state-of-the-art. Redox Biol. 2021 Jun;42:101872.
5. Chauhan LK, Pant N, Gupta SK, Srivastava SP. Induction of chromosome aberrations, micronucleus formation and sperm abnormalities in mouse following carbofuran exposure. Mutat Res. 2000 Feb 16;465(1-2):123-9.
6. Cohen G, Dembiec D, Marcus J. Measurement of catalase activity in tissue extracts. Anal Biochem. 1970,34:30-8.
7. Das S, Das J, Paul A, Samadder A, Khuda-Bukhsh AR. Apigenin, a bioactive flavonoid from Lycopodium clavatum, stimulates nucleotide excision repair genes to protect skin keratinocytes from ultraviolet B-induced reactive oxygen species and DNA damage. J Acupunct Meridian Stud. 2013 Oct;6(5):252-62.
8. Gray P. The Microtomist's Formulary and Guide. Blakiston. New York. 1954;43(8):403–409.
9. Gupta RK, Pandey R, Sharma G, Prasad R, Koch B, Srikrishna S, et al. DNA binding and anti-cancer activity of redox-active heteroleptic piano-stool Ru(II), Rh(III), and Ir(III) complexes containing 4-(2-methoxypyridyl)phenyldipyrromethene. Inorg Chem. 2013 Apr 1;52(7):3687-98.
10. Hassan SM, Khalaf MM, Sadek SA, Abo-Youssef AM. Protective effects of Apigenin and myricetin against cisplatin-induced nephrotoxicity in mice. Pharm Biol. 2017 Dec;55(1):766-774.
11. Healy EF. Quantitative determination of DNA–ligand binding using fluorescence spectroscopy, J. Chem. Educ. 2007;84:1304–1307.
12. Islam BU, Habib S, Ahmad P, Allarakha S, Moinuddin, Ali A. Pathophysiological Role of Peroxynitrite Induced DNA Damage in Human Diseases: A Special Focus on Poly(ADP-ribose) Polymerase (PARP). Indian J Clin Biochem. 2015 Oct;30(4):368-85.
13. Kang J, Wu H, Lu X, Wang Y, Zhou L. Study on the interaction of new water-soluble porphyrin with DNA. Spectrochim. Acta A. 2005;61:2041.
14. Khan MA, Singh D, Fatma H, Akhtar K, Arjmand F, Maurya S, Siddique HR. Antiandrogen enzalutamide induced genetic, cellular, and hepatic damages: amelioration by triterpene Lupeol. Drug

Chem Toxicol. 2022 Feb 21:1-12.

15. Lathia C, Lettieri J, Cihon F, Gallentine M, Radtke M, Sundaresan P. Lack of effect of ketoconazole-mediated CYP3A inhibition on sorafenib clinical pharmacokinetics. Cancer Chemother. Pharmacol. 2006;57(5):685–92.
16. Li Y, Gao ZH, Qu X.J. The adverse effects of Sorafenib in patients with advanced cancers. Basic Clin Pharmacol Toxicol. 2015 Mar;116(3):216-21.
17. Liou GY, Storz P. Reactive oxygen species in cancer. Free Radic Res. 2010 May;44(5):479-96.
18. Liu L, Cao Y, Chen C, Zhang X, McNabola A, Wilkie D, et al. Sorafenib blocks the RAF/MEK/ERK pathway, inhibits tumor angiogenesis, and induces tumor cell apoptosis in hepatocellular carcinoma model PLC/PRF/5. Cancer Res. 2006 Dec 15;66(24):11851-8.
19. Liu R, Ji P, Liu B, Qiao H, Wang X, Zhou L, et al. Apigenin enhances the cisplatin cytotoxic effect through p53-modulated apoptosis. Oncol Lett. 2017 Feb;13(2):1024-1030.
20. Llovet JM, Ricci S, Mazzaferro V, Hilgard P, Gane E, Blanc JF, et al. Sorafenib in advanced hepatocellular carcinoma. N Engl J Med. 2008; 359:378–390
21. Marklund S, Marklund G. Involvement of the superoxide anion radical in the autoxidation of pyrogallol and a convenient assay for superoxide dismutase. Eur J Biochem. 1974 Sep 16;47(3):469-74.
22. Marmur J, Doty P. Thermal renaturation of deoxyribonucleic acids. J Mol Biol. 1961 Oct;3:585-94.
23. Maurya SK, Shadab GGHA, Siddique HR. Chemosensitization of Therapy Resistant Tumors: Targeting Multiple Cell Signaling Pathways by Lupeol, A Pentacyclic Triterpene. Curr Pharm Des. 2020;26(4):455-465.
24. McGill MR. The past and present of serum aminotransferases and the future of liver injury biomarkers. EXCLI J. 2016 Dec 15;15:817-828.
25. Meadows KA, Liu F, Sou J, Hudson BP, McMillin DR. Spectroscopic and photophysical studies of the binding interactions between copper phenanthroline complexes and RNA. Inorg. Chem. 1993; 32: 2919–2923.
26. Niknahad H, Heidari R, Mohammadzadeh R, Ommati MM, Khodaei F, Azarpira N, et al. Sulfasalazine induces mitochondrial dysfunction and renal injury. Ren Fail. 2017 Nov;39(1):745-753.
27. Norma P. MelÃ©ndez, Virginia NevÃ¡rez-MoorillÃ³n RaÃºl, RodrÃguez-Herrera JosÃ© C, Espinoza CristÃ³bal N, Aguilar. A microassay for quantification of 2,2-diphenyl-1-picrylhydracyl (DPPH) free radical scavenging. African Journal of Biochemistry Research. 2014: 8(1): 14-18
28. Pal MK, Jaiswar SP, Dwivedi A, Goyal S, Dwivedi VN, Pathak AK, et al. Synergistic Effect of Graphene Oxide Coated Nanotised Apigenin with Paclitaxel (GO-NA/PTX): A ROS Dependent Mitochondrial Mediated Apoptosis in Ovarian Cancer. Anti-cancer Agents Med Chem. 2017;17(12):1721-1732.
29. Parveen S, Tabassum S, Arjmand F. Synthesis of chiral: R / S -pseudopeptide-based Cu(II) & Zn(II) complexes for use in targeted delivery for antitumor therapy: Enantiomeric discrimination with CT-DNA and pBR322 DNA hydrolytic cleavage mechanism. RSC Adv. 2017;6587–6597.

30. Raja A, Rajendiran V, Uma Maheswari P, Balamurugan R, Kilner CA, Halcrow MA, et al. Copper(II) complexes of tridentate pyridylmethylethylenediamines: role of ligand steric hindrance on DNA binding and cleavage. J Inorg Biochem. 2005 Aug;99(8):1717-32.
31. Rotruck JT, Pope AL, Ganther HE, Swanson AB, Hafeman DG, Hoekstra WG. Selenium: biochemical role as a component of glutathione peroxidase. Science. 1973 Feb 9;179(4073):588-90.
32. Siddique HR, Mishra SK, Karnes RJ, Saleem M. Lupeol, a novel androgen receptor inhibitor: implications in prostate cancer therapy. Clin Cancer Res. 2011 Aug 15;17(16):5379-91.
33. Singh D, Khan MA, Siddique HR. Apigenin, A Plant Flavone Playing Noble Roles in Cancer Prevention Via Modulation of Key Cell Signaling Networks. Recent Pat Anticancer Drug Discov. 2019;14(4):298-311.
34. Somade OT, Ugbaja RN, Alli AA, Odubote OT, Yusuf TS, Busari BT, et al. Diallyl disulfide, an organo-sulfur compound in garlic and onion attenuates trichloromethane-induced hepatic oxidative stress, activation of NFkB and apoptosis in rats. J. Nutrition & Intermediary Metabolism. 2018;13:10-19.
35. Storz P. Reactive oxygen species in tumor progression. Front Biosci. 2005 May 1;10:1881-96.
36. Tan LF, Chao H, Zhen KC, Fei JJ, Wang F, Zhou YF, et al. Synthesis and characterization of Co(ii) and Fe(ii) peptide conjugates as hydrolytic cleaving agents and their preferential enantiomeric disposition for CT-DNA: structural investigation of l-enantiomers by DFT and molecular docking studies. *Polyhedron,* 2007, **26**: 5458.
37. Tao G, Huang J, Moorthy B, Wang C, Hu M, Gao S, et al. Potential role of drug metabolizing enzymes in chemotherapy-induced gastrointestinal toxicity and hepatotoxicity. Expert Opin Drug Metab Toxicol. 2020 Nov;16(11):1109-1124.
38. Ting CT, Cheng YY, Tsai TH. Herb-Drug Interaction between the Traditional Hepatoprotective Formulation and Sorafenib on Hepatotoxicity, Histopathology and Pharmacokinetics in Rats. Molecules. 2017 Jun 22;22(7):1034.
39. Wang F, Liu JC, Zhou RJ, Zhao X, Liu M, Ye H, et al. Apigenin protects against alcohol-induced liver injury in mice by regulating hepatic CYP2E1-mediated oxidative stress and PPARα-mediated lipogenic gene expression. Chem Biol Interact. 2017 Sep 25;275:171-177.
40. Williet N, Clavel L, Bourmaud A, Verot C, Bouarioua N, Roblin X, et al. Tolerance and outcomes of Sorafenib in elderly patients treated for advanced hepatocellular carcinoma. Dig Liver Dis. 2017 Sep;49(9):1043-1049.
41. Wolfe A, Shimer Jr GH, Meehan T. Polycyclic aromatic hydrocarbons physically intercalate into duplex regions of denatured DNA. Biochemistry. 1987; 26:6392–6396.
42. Yan X, Qi M, Li P, Zhan Y, Shao H. Apigenin in cancer therapy: anti-cancer effects and mechanisms of action. Cell Biosci. 2017 Oct 5;7:50.

Figures

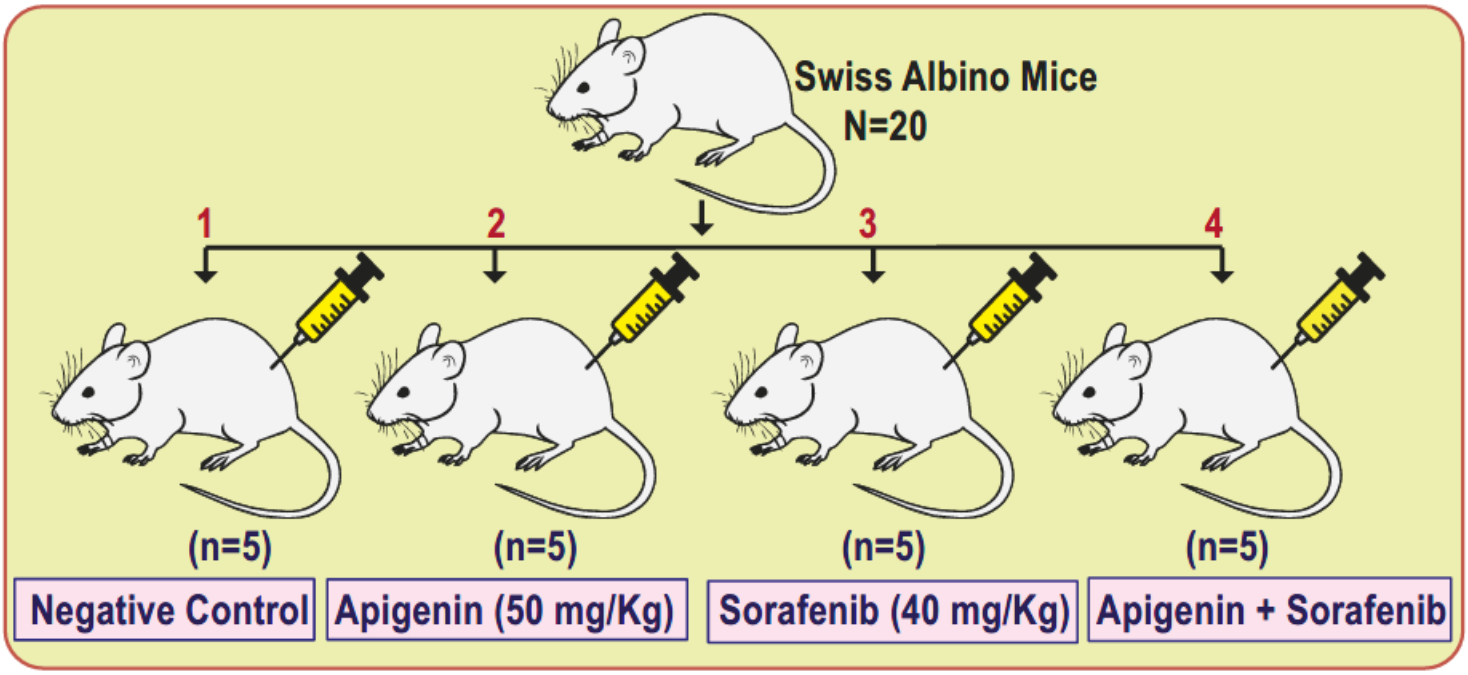

Figure 1

Schematic illustration of the experimental design for *in vivo* experiments.

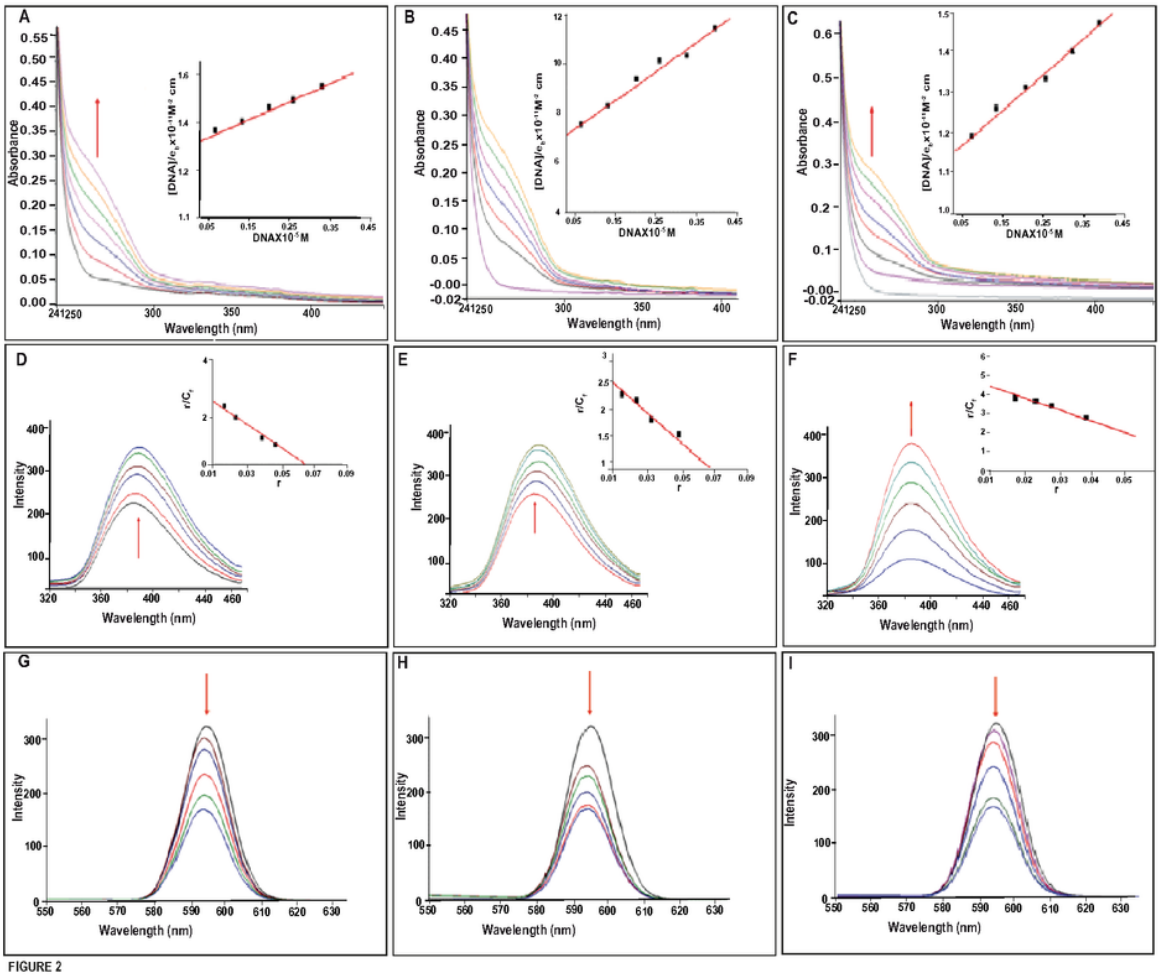

Figure 2

Absorption spectra of the compounds; Apigenin **(A)**, Sorafenib **(B)**, Apigenin + Sorafenib **(C)** in Tris–HCl buffer on progressive addition of ct-DNA at 25 ºC. Inset: plot of (DNA)/ε_b vs. (DNA) for the titration of ct-DNA with the compound, (Apigenin, Sorafenib and Apigenin + Sorafenib)= 6.66 x 10^{-6} M, (DNA)= 0–3.33 x 10^{-5} M. The emission spectra of the compounds Apigenin **(D)**, Sorafenib **(E)**, Apigenin + Sorafenib **(F)**. Ethidium bromide displacement or quenching experiment of the compounds Apigenin **(G)**, Sorafenib **(H)**, Apigenin + Sorafenib **(I)**.

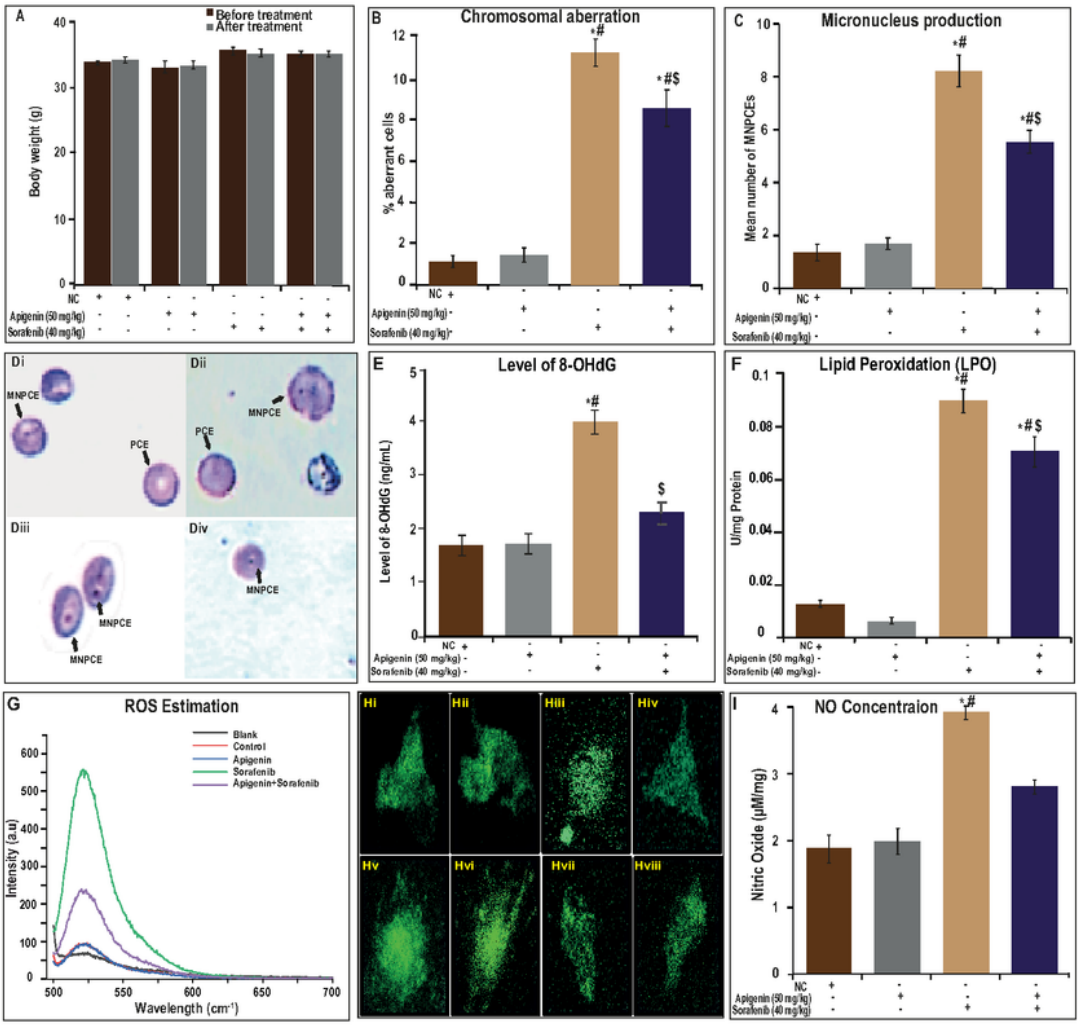

FIGURE 3

Figure 3

Effect of Apigenin, Sorafenib, and Combination treatment on body weight of animals **(A)**. Bar graph representing the protective role of Apigenin against Sorafenib induced chromosomal aberrations and micronucleus production in the bone marrow cells of mice **(B-C)**. Photomicrographs representing the Sorafenib induced micronucleus production **(Di-iv)**. Bar graph representing Sorafenib induced increase in 8-OHdG and MDA levels (**E-F**), Sorafenib induced ROS and Nitric oxide production in the liver **(G-I)**. Results

are expressed as the Mean ± SD (n=5), ($p < 0.05$). Data were analyzed by one-way ANOVA followed by Tukey's post hoc test for multiple comparisons. * Significant difference in comparison with the control group. # Significant difference in comparison with the Apigenin treated group. $ Significant difference in comparison to the Sorafenib treated group. Hi-ii: control; Hiii-iv: Apigenin; Hv-vi: Sorafenib; Hvii-viii: Apigenin+Sorafenib

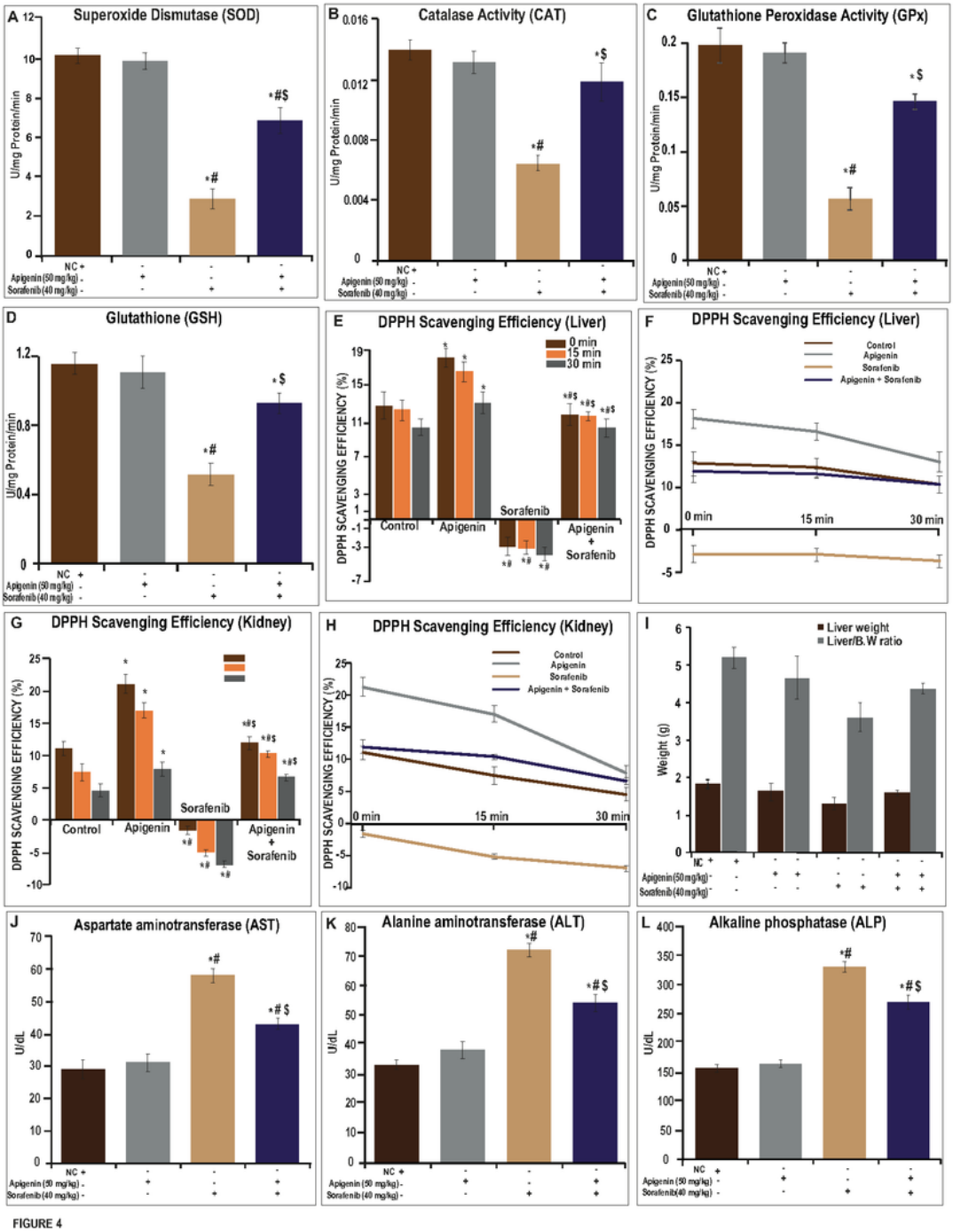

FIGURE 4

Figure 4

Bar graph representing Sorafenib induced decrease in the SOD, CAT, GPX, and GSH levels and the mitigating role of Apigenin against this oxidative damage **(A-D)**, % DPPH scavenging activity (**E-H**), Effect of Apigenin, Sorafenib, and Combination treatment on liver weight and liver to body weight ratio (**I**). Bar graph representing changes in the serum levels of Aspartate aminotransferase (AST) (**J**), Alanine aminotransferase (ALT) (**K**) Alkaline phosphatase (ALP) (**L**) on Sorafenib treatment for 48 hrs. Further, combination treatment with Apigenin and Sorafenib improved the functioning of the liver in the treated animals and shifted the liver function markers towards normal. Results are expressed as the Mean ± SD (n=5), ($p < 0.05$). Data were analyzed by one-way ANOVA followed by Tukey's post hoc test for multiple comparisons. * Significant difference in comparison with the control group. # Significant difference in comparison with the Apigenin treated group. $ Significant difference in comparison to the Sorafenib treated group.

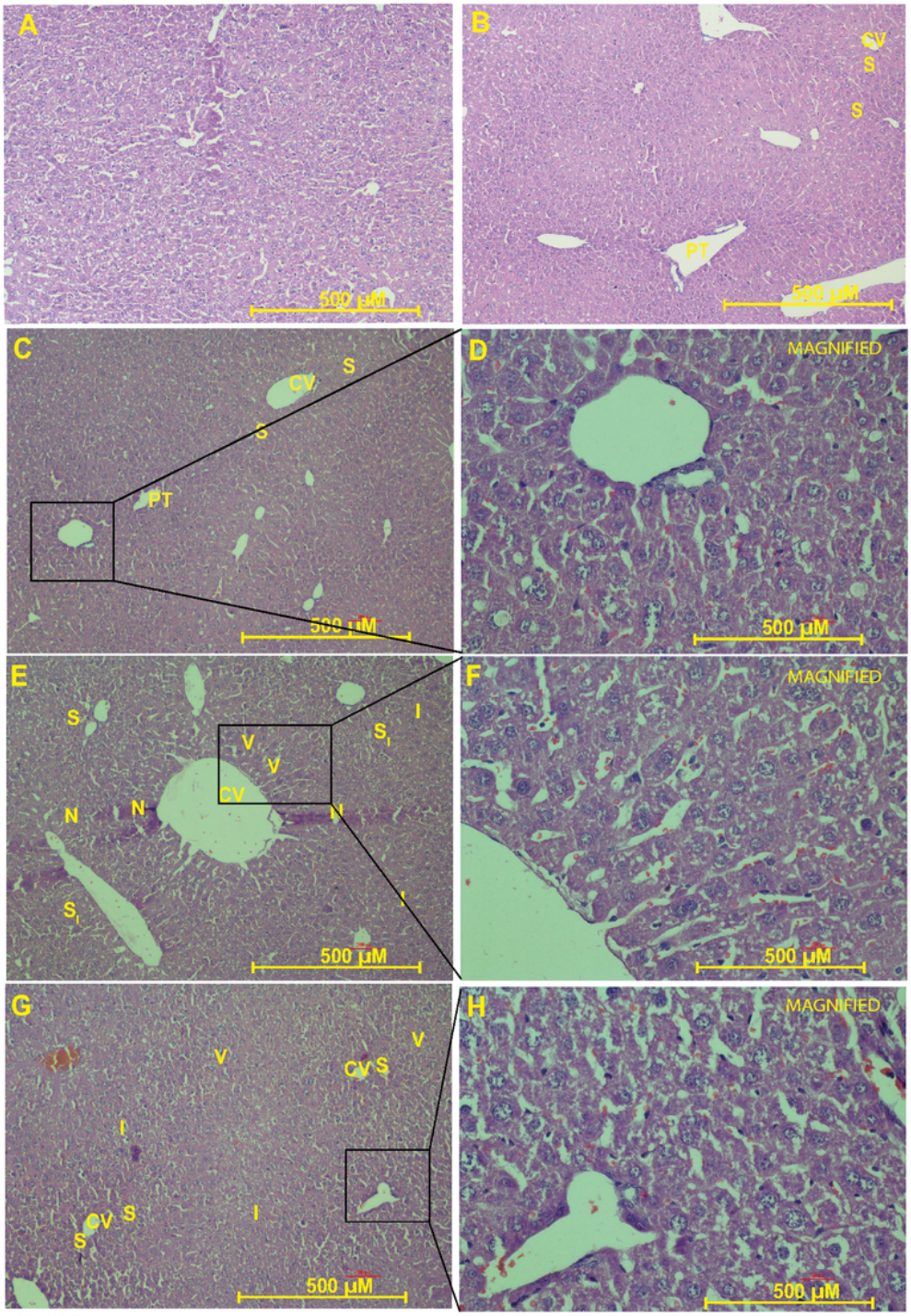

FIGURE 5

Figure 5

Histopathological observations of the liver sections stained with Haematoxylin & Eosin showing Apigenin's hepatoprotective effects on the Sorafenib-induced abnormalities in the liver as revealed by a reduction in the severity of lesions and restoration of the normal histology (**A-H**). D, F, and H are higher power magnification pictures.

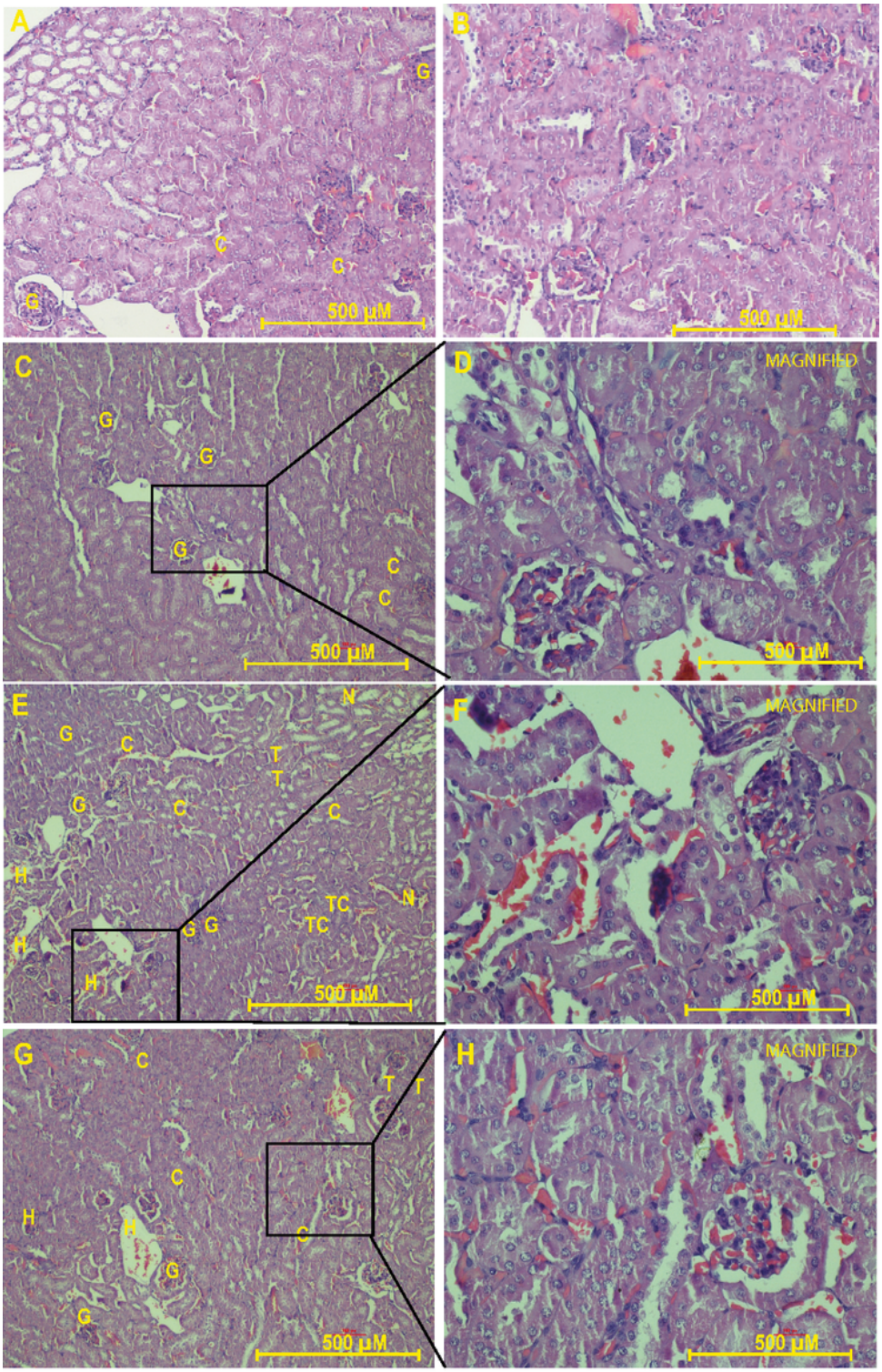

FIGURE 6

Figure 6

Histopathological observations of kidney sections stained with Haematoxylin & Eosin showing Apigenin's protective effects on the Sorafenib induced abnormalities in the kidney as revealed by a reduction in the

severity of lesion and restoration of the renal histology towards normal (**A-H**). D, F, and H are higher power magnification pictures.

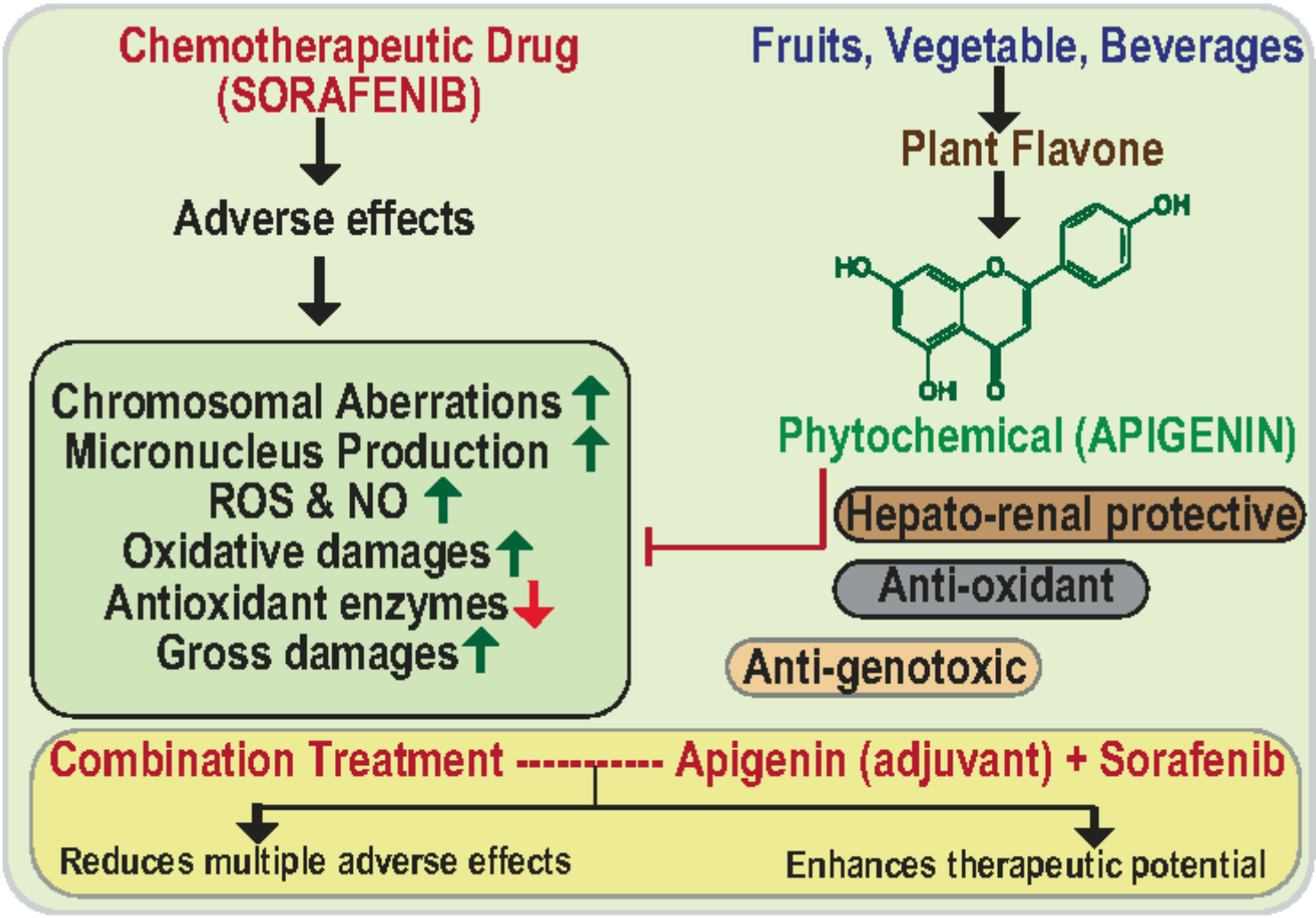

Figure 7

Figure 7

An illustration of the proposed mechanism of Sorafenib-induced toxicity and the protective effects of Apigenin.

Supplementary Files

This is a list of supplementary files associated with this preprint. Click to download.

- GraphicalAbstract.eps